Naval Research Laboratory

Washington, DC 20375-5320

NRL/MR/6355--15-9583

Effect of Crack Tip Stress Concentration Factor on Fracture Resistance in Vacuum Environment

P.S. Pao
R.L. Holtz

Multifunctional Materials Branch
Materials Science and Technology Division

January 20, 2015

REPORT DOCUMENTATION PAGE

Form Approved
OMB No. 0704-0188

1. REPORT DATE *(DD-MM-YYYY)*	**2. REPORT TYPE**	**3. DATES COVERED** *(From - To)*
20-01-2015	Memorandum Report	October 2011 – September 2014

4. TITLE AND SUBTITLE

Effect of Crack Tip Stress Concentration Factor on Fracture Resistance in Vacuum Environment

5a. CONTRACT NUMBER

5b. GRANT NUMBER

5c. PROGRAM ELEMENT NUMBER

6. AUTHOR(S)

P.S. Pao and R.L. Holtz

5d. PROJECT NUMBER

5e. TASK NUMBER

5f. WORK UNIT NUMBER
63-2634-A4

7. PERFORMING ORGANIZATION NAME(S) AND ADDRESS(ES)

Naval Research Laboratory
4555 Overlook Avenue, SW
Washington, DC 20375-5328

8. PERFORMING ORGANIZATION REPORT NUMBER

NRL/MR/6355--15-9583

9. SPONSORING / MONITORING AGENCY NAME(S) AND ADDRESS(ES)

Office of Naval Research
One Liberty Center
875 North Randolph Street, Suite 1425
Arlington, VA 22203-1995

10. SPONSOR / MONITOR'S ACRONYM(S)

ONR

11. SPONSOR / MONITOR'S REPORT NUMBER(S)

12. DISTRIBUTION / AVAILABILITY STATEMENT

Approved for public release; distribution is unlimited.

13. SUPPLEMENTARY NOTES

14. ABSTRACT

An investigation was carried out to characterize the effect of crack tip stress concentration factor (K_t) on fracture resistance of various aluminum alloys and a steel in vacuum environment. The materials investigated were peakaged 7075-T651, overaged 7075-T7351, 5083-H131, fully sensitized Al 5083 (175°C/240 hrs), 2024-T351, and AISI 4340 steel. Fracture mechanics wedge-opening-load (WOL) specimens were used in the current study. The test environment was vacuum so that the baseline fracture resistance of the material without the influence of environment could be determined. The results indicate: (1) in all alloys, the fracture resistance is highest for blunt-notches (smaller K_t), and is lowest for fatigue-sharpened precracked notches (larger K_t); (2) the fracture resistance decreases linearly as K_t increases; (3) at similar K_t levels, AISI 4340 steel exhibits fracture resistance about twice higher than those of the aluminum alloys; (4) the peakaged 7075-T651 and overaged 7075-T7351 have comparable fracture resistance; (5) the fracture resistance of 2024-T351 alloy is higher than 7075 alloys; (6) the fracture resistances of as-received 5083-H131 (5083R) and sensitized 5083S (175°C/240 hrs) are comparable in all K_t, except at the smallest $K_t = 3$ where the fracture resistance of 5083R is higher; and (7) the fracture paths are transgranular and the fracture mode is ductile void coalescence in all cases, irrespective of the stress concentration factor.

15. SUBJECT TERMS

Stress concentration factor
Steel
Aluminum alloys
Fracture

16. SECURITY CLASSIFICATION OF:			**17. LIMITATION OF ABSTRACT**	**18. NUMBER OF PAGES**	**19a. NAME OF RESPONSIBLE PERSON**
a. REPORT	**b. ABSTRACT**	**c. THIS PAGE**			Peter S. Pao
Unclassified Unlimited	Unclassified Unlimited	Unclassified Unlimited	Unclassified Unlimited	17	**19b. TELEPHONE NUMBER** *(include area code)* (202) 767-0224

Contents

Introduction 1

Experimental Procedure 1

Results and Discussion 2
Effect of Stress Concentration Factor 2
SEM Fractographic Examination 3

Conclusions 3

References 5

Appendix A – Figures 6

ACKNOWLEDGMENTS

The authors gratefully acknowledge the support from Office of Naval Research (ONR), Arlington, VA, monitored by Dr. Lawrence Kabacoff. The author wishes to express his appreciation to Dr. A.K. Vasudevan, formerly with ONR, for his helpful discussions, to Dr. C.R. Feng for his assistance in SEM fractographic examination, and to Dr. F. Bovard of Alcoa for providing Al 5083-H131 plates.

INTRODUCTION

The presence of cracks in engineering structures can significantly raise the local crack tip stresses and reduce the load-carrying capability of the structures. The extent of crack tip stress increases depends on the geometry and the sharpness of the crack. The sharpness of the crack tip stresses can be defined by a dimensionless term called "stress concentration factor", K_t, which is defined as the ratio of the highest stress in the element to the nominal stress.

$$K_t = \sigma_{max} / \sigma_n \quad (1)$$

Nominal stress represents the total stress within an element under the same loading conditions but without the cracks (stress concentrators). That is, the nominal stress computations assume that the components are smooth and uniform with no irregularities. If the component is flawless and has no irregularities, then the stress concentration factor, K_t, equals to 1. For all other components that contain flaws, K_t would be grater than 1, with larger K_t corresponding to a sharper crack.

However, in many structural components, flaws and cracks are either present due to material and/or machining defects or develop during service because of corrosion and/or various loading conditions such as fatigue, fretting, abrasion, etc. Also, the geometry of the structure may cause an increase in K_t. Thus, systematic determinations of the influence of K_t on the fracture stress intensity factor K_q for various engineering materials are required for the construction of Goodman diagrams for life prediction analyses. Because the effect of cracks and stress concentration can be enhanced by the presence of aggressive environments (via stress-corrosion cracking and/or corrosion-fatigue), it is necessary to establish the K_t effect in an inert environment such as in vacuum, so that the true material's resistance to fracture at various K_t can be established as a reference.

In this study, the effect of K_t on the fracture stress intensity factor, K_q, of AISI 4340 steel, peakaged Al 7075-T651, overaged Al 7075-T7351, Al 5083-H131, and sensitized Al 5083-H131 (175°C/240 hrs) are determined in a vacuum environment. The K_t varies from a low of 3 for a blunt notch to over 50 for a fatigue-sharpened precrack. The results are compiled in this report.

EXPERIMENTAL PROCEDURE

The materials used in this study were (1) 2.54-mm thick AISI 4340 steel, (2) 63.5-mm thick 7075-T651, (3) 63.5-mm thick 7075-T7351, (4) 58.4-mm thick 5083-H131 (designated as 5083R), (5) 58.4-mm thick 5083-H131 sensitized at 175°C/240 hrs (designated as 5083S), and (6) 63.5-mm thick 2024-T351 plates.

For fracture resistance as a function of K_t studies, wedge-opening-load (WOL) fracture mechanics specimens, were used. The specimen orientation for AISI 4340 was LT, for 5083R and 5083S are SL, and for 7075-T651, 7075-T7351, and 2024-T351 were ST. The stress-intensity factor (K) for the WOL specimens was computed from the relationship

Manuscript approved November 14, 2014.

(references 1 - 2):

$$K = [P/(BW^{1/2})]\,[(2 + a/W)(0.8072 + 8.858\,(a/W) - 30.23\,(a/W)^2 + 41.088\,(a/W)^3 - 24.15\,(a/W)^4 + 4.951\,(a/W)^5]/(1 - a/W)^{3/2}, \quad (2)$$

where P = applied load, B = specimen thickness, W = specimen width, and a = crack length. The notch tip radii (ρ) at the crack tip range from 3.175 mm, 0.787 mm, 0.254 mm, 0.127 mm, 0.076 mm, and fatigue-sharpened precrack. The notch radius of 0.076 mm is the smallest radius that can be machined using a conventional carbide cutter. The fatigue-sharpened precrack represents the lower limit of notch crack radius.

The relationship between the local maximum stress at the notch tip (σ_{max}) and stress intensity, K, is below.

$$\sigma_{max} = 2\,K / (\pi\,\rho)^{1/2} \quad (3)$$

For the WOL specimen, the nominal stress at the notch tip (σ_n) is giving by:

$$\sigma_n = P\,[1 + 3\,((W + a) / (W - a))] / [B\,(W - a)] \quad (4)$$

Then stress concentration factor, K_t, thus can be computed from Eq. 1.

All fracture resistance tests are conducted in vacuum ($< 6 \times 10^{-6}$ Pa background pressure) at ambient temperature (20°C). The step-load test method was used to determine the effect of K_t in AISI 4340 steel and in 7075-T651. In addition, continuous loading program developed by Fracture Technology Associates (FTA) in accordance to ASTM E399 was used for 7075-T651, 7075-T651, 2024-T351, 5083R, and 5083S (reference 3). After fracture resistance tests, selected 7075-T651 and 7075-T7351 fracture surfaces were studied by scanning electron microscopy (SEM).

RESULTS AND DISCUSSION

EFFECT OF STRESS CONCENTRATION FACTOR

The effects of stress concentration factor, K_t, on the fracture resistance, K_q, for AISI 4340 steel, 7075-T651, 7075-T7351, 2024-T351, as-received 5083-H131 (5083R), and sensitized 5083-H131 (5083S) are shown in Figs. A-1 – A-9. In all alloys, the K_q is highest for blunt-notches (smaller K_t), and is lowest for fatigue-sharpened precracked notches (larger K_t). The fracture resistance, K_q, decrease linearly as K_t increases from 3 to 40.

The K_q in AISI 4340 steel, as shown in Fig. A-1, is more than twice higher, at a comparable K_t, than aluminum alloys, as shown in Figs. A-2 through A-9. This is because AISI 4340 steel has significantly higher strength than aluminum alloys. In AISI 4340 steel, the fracture resistance at a very high K_t of 40 is about 110 MPa$\sqrt{m}$, which is significantly higher than any of the blunt-notched aluminum alloys. The fracture

resistance of fatigue-sharpened AISI 4340 steel is around 70 MPa√m, which is significantly lower than the K_q at K_t of 40 but is comparable to the K_q of blunt-notched aluminum alloys.

The fracture resistance, K_q, for all aluminum alloys is between 30 and 80 MPa√m, for K_t ranging from about 3 (blunt) to fatigue-sharpened specimens. The fracture resistance of fatigue-sharpened aluminum alloys are comparable to the K_q of smallest machined notch specimens (K_t = 20).

As shown in Fig. A-4, the effect of stress concentration on fracture resistance of 7075-T651 was determined using both step-loading and continuous loading FTA test program. Data in Fig. A-4 indicates that there is little difference between these two methodologies.

Figure A-6 compares the fracture resistance of peakaged 7075-T651 and overaged 7075-T7351 as a function of stress concentration, K_t. As shown in Fig. A-6, the fracture resistances of these two aluminum alloys are comparable at each K_t.

The fracture resistances of 2024-T351 and peakaged 7075-T651 at various K_t are compared in Fig. A-8. As shown in Fig. A-8, the fracture resistance of 2024-T351 is about 10 MPa√m higher than that of 7075-T651 in all K_t, except at the smallest K_t =3 where the fracture resistance of these two alloys are comparable. The higher fracture resistance in 2024-T351 is probably due to its lower strength and higher ductility, when compared to peakaged 7075-T651.

The fracture resistances of as-received 5083-H131 (5083R) and sensitized 5083S (175°C/240 hrs) are compared in Fig. A-9. As shown in Fig. A-9, the fracture resistance of 5083R and 5083S are comparable in all K_t, except at the smallest K_t =3 where the fracture resistance of 5083R is higher.

SEM FRACTOGRAPHIC EXAMINATION

The fracture surface morphology was examined by scanning electron microscopy (SEM). In inert vacuum environment, the fracture paths are transgranular and the fracture mode is ductile void coalescences in all cases, irrespective of the stress concentration factor. Examples of these ductile void coalescences fracture surface morphologies are shown at low and high K_t for 7075-T651 in Fig. A-10 and for 7075-T7351 in Fig. A-11. As shown in Figs. A-10 and 11, the predominant fracture mode at the notch tip is ductile void coalescence.

CONCLUSIONS

The effect of crack tip stress concentration factor on fracture resistance of AISI 4340 steel, 7075-T651, 7075-T7351, 2024-T351, 5083-H131, and sensitized 5083 (175°C/240 hrs) were determined in inert vacuum environment. In all alloys, the fracture resistance was highest for blunt-notches (smaller K_t), and was lowest for fatigue-sharpened precracked notches (larger K_t). The fracture resistance decreased linearly as K_t increased.

Because of its high strength, AISI 4340 steel exhibits fracture resistance about twice higher than those of the aluminum alloys, at similar K_t levels. The peakaged 7075-T651 and overaged 7075-T7351 have comparable fracture resistance, even though peakaged 7075-T651 is about 14% stronger than overaged 7075-T7351. The fracture resistance of 2024-T351 alloy is higher than 7075 alloys because of its higher ductility and significantly lower strengths. Finally, the fracture resistances of as-received 5083-H131 (5083R) and sensitized 5083S (175°C/240 hrs) are comparable in all K_t, except at the smallest K_t =3 where the fracture resistance of 5083R is higher.

The fracture surface morphology was examined by scanning electron microscopy (SEM). In inert vacuum environment, the fracture paths are transgranular and the fracture mode is ductile void coalescence in all cases, irrespective of the stress concentration factor.

REFERENCES

1. Ashok Saxena and S.J. Hudak, Jr., Int. J. Fract., 1978, Vol. 14, pp. 453-468.

2. R.P. Wei, P.S. Pao, R.G. Hart, T.W. Weir, and G.W. Simmons, “Fracture Mechanics and Surface Chemistry Studies of Fatigue Crack Growth in an Aluminum Alloy,” *Metall. Trans. A.* Vol. 11A, 1980, pp. 151-158.

3. *Standard Test Method for Plane-Strain Fracture Toughness of Metallic Materials, ASTM E 399-06*, ASTM International, (2006).

APPENDIX A
FIGURES

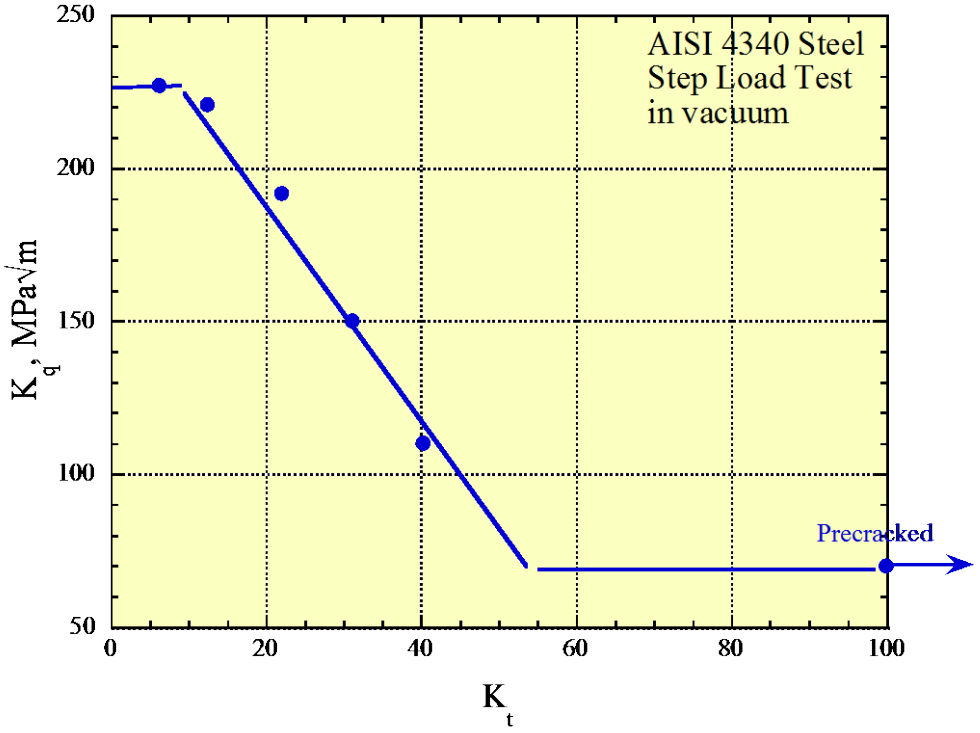

Figure A-1: Effect of K_t on fracture resistance of AISI 4340 steel.

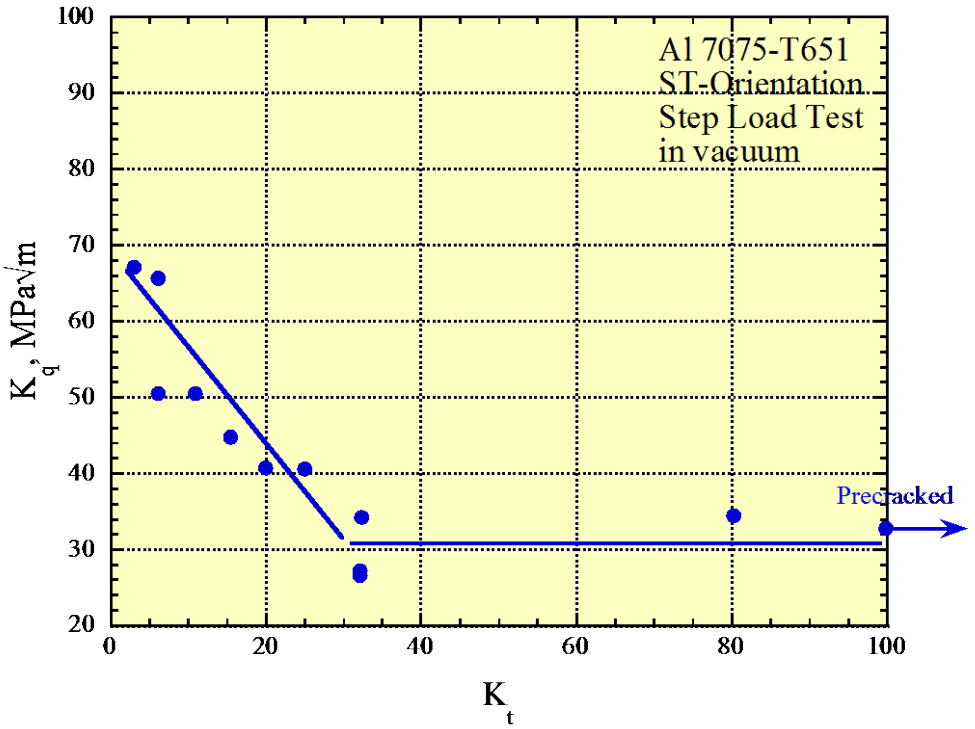

Figure A-2: Effect of K_t on fracture resistance of Al 7075-T651 (step load test).

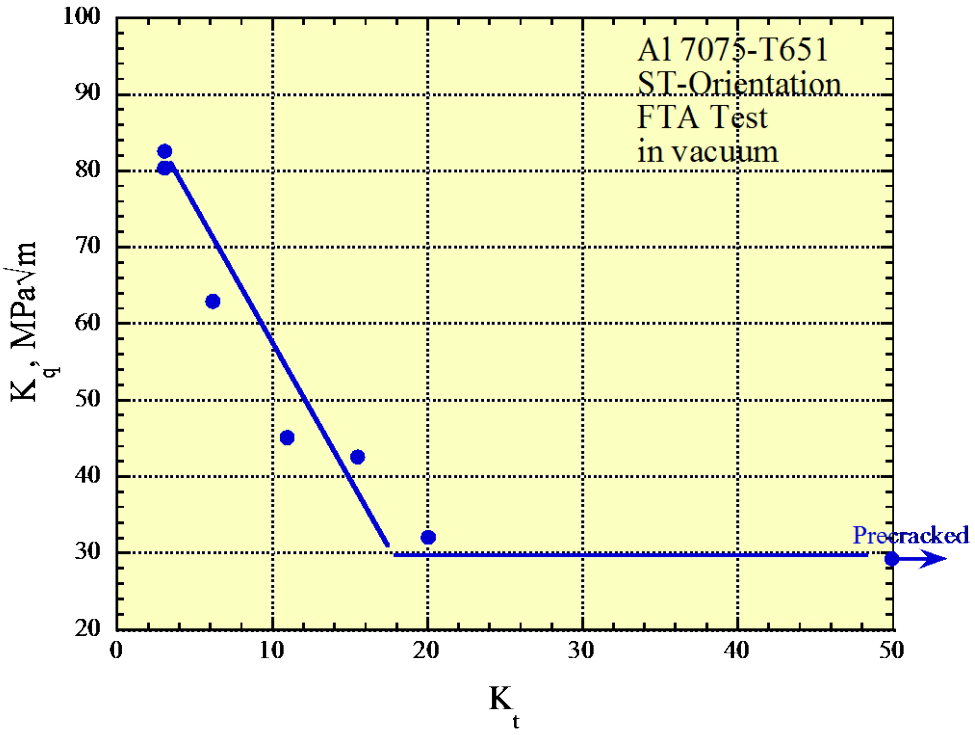

Figure A-3: Effect of K_t on fracture resistance of Al 7075-T651 (FTA test).

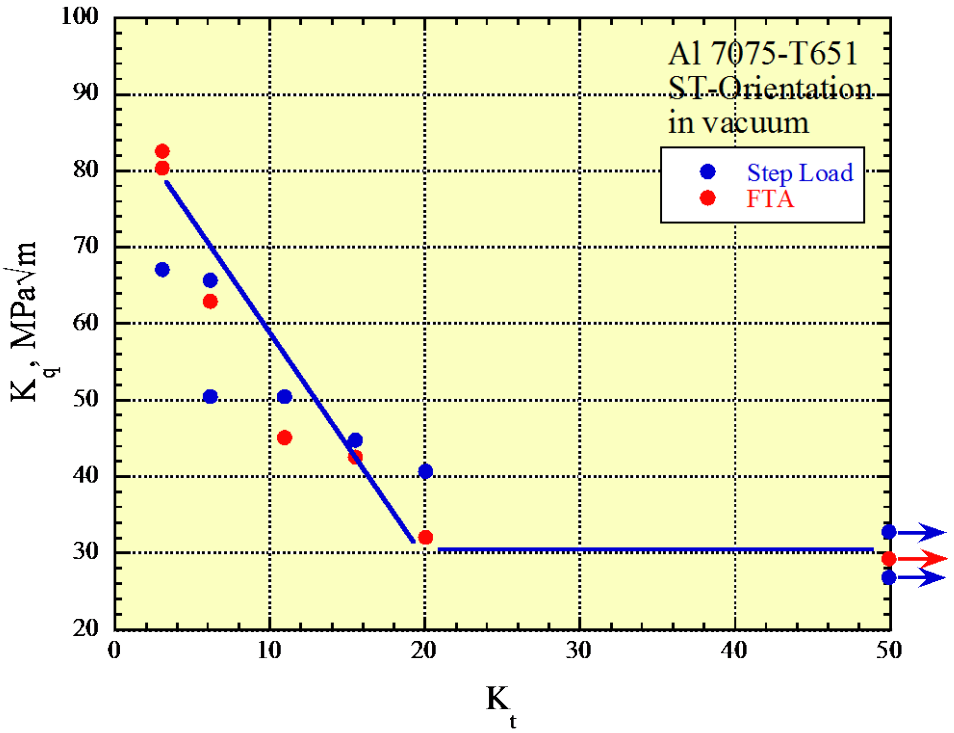

Figure A-4: Effect of K_t on fracture resistance of Al 7075-T651 (step load and FTA tests).

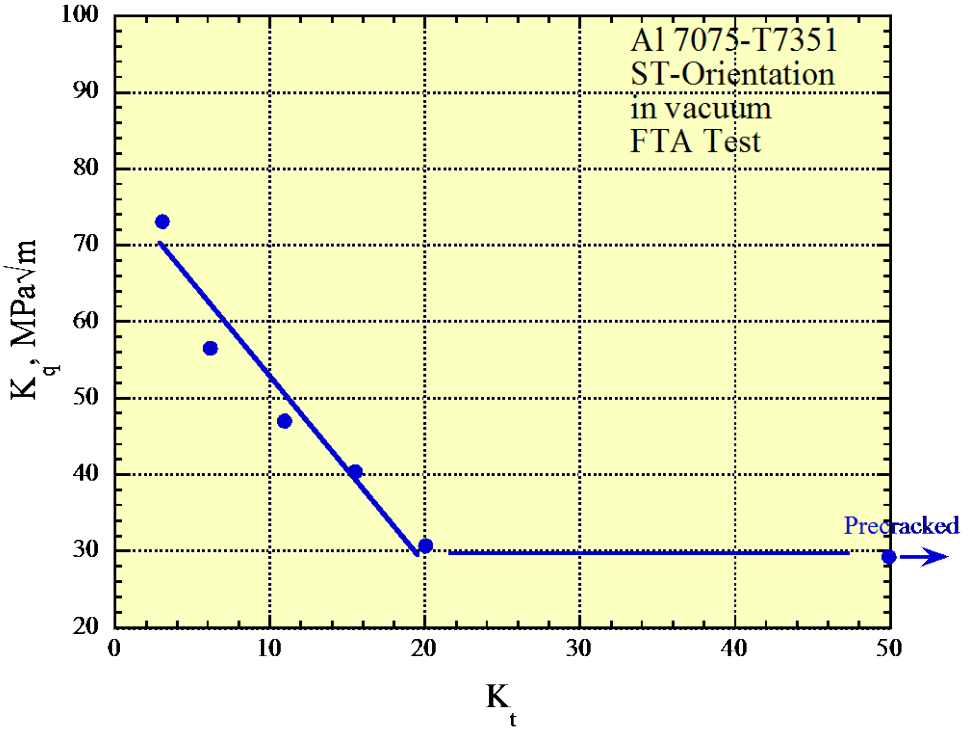

Figure A-5: Effect of K_t on fracture resistance of Al 7075-T7351 (FTA test).

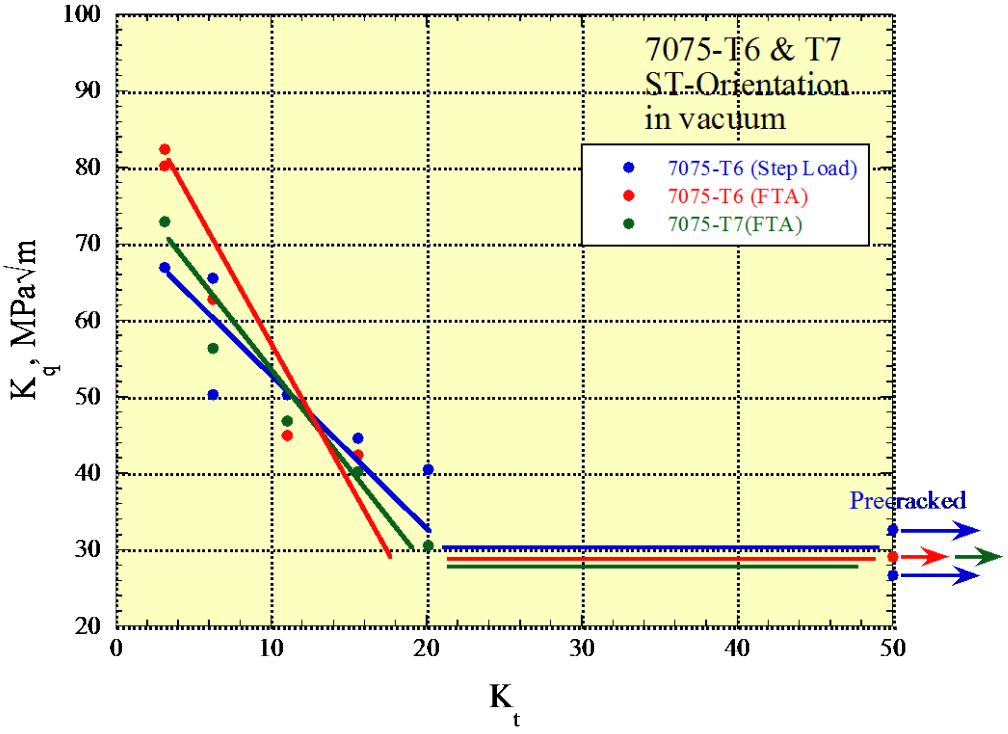

Figure A-6: Effect of K_t on fracture resistance of Al 7075-T651 and Al 7075-T7351.

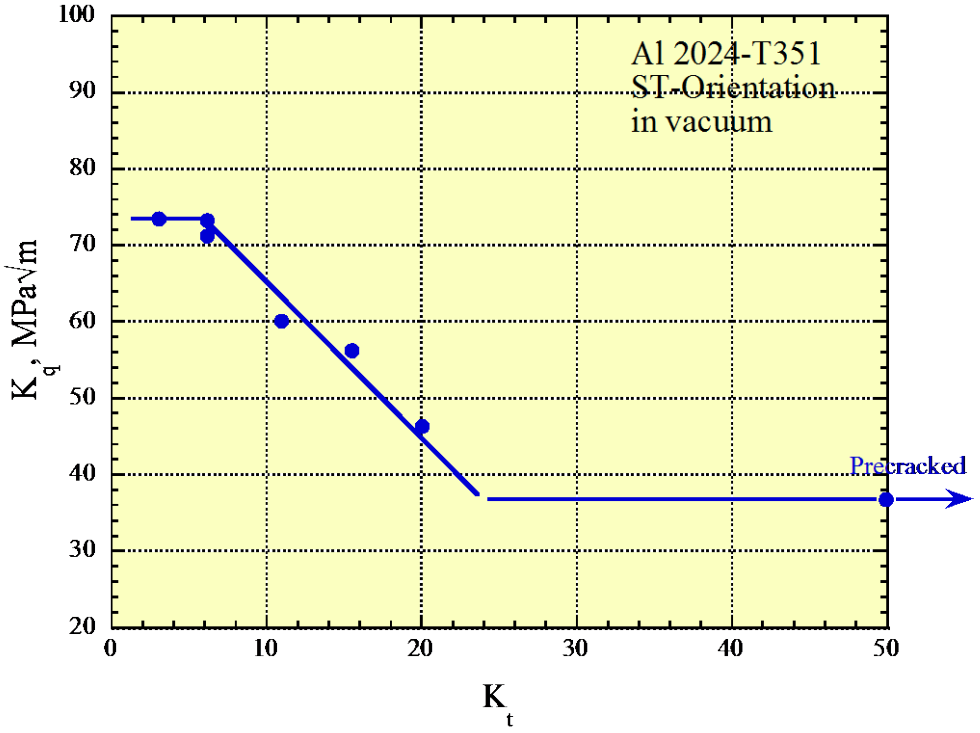

Figure A-7: Effect of K_t on fracture resistance of Al 2024-T351.

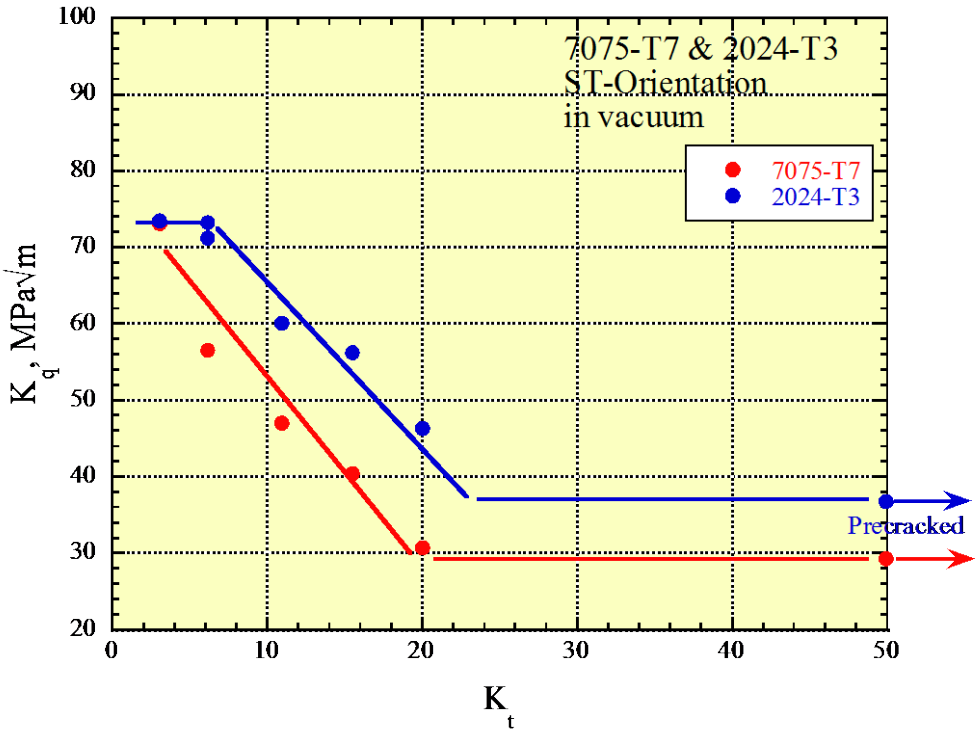

Figure A-8: Effect of K_t on fracture resistance of Al 2024-T351 and Al 7075-T7351.

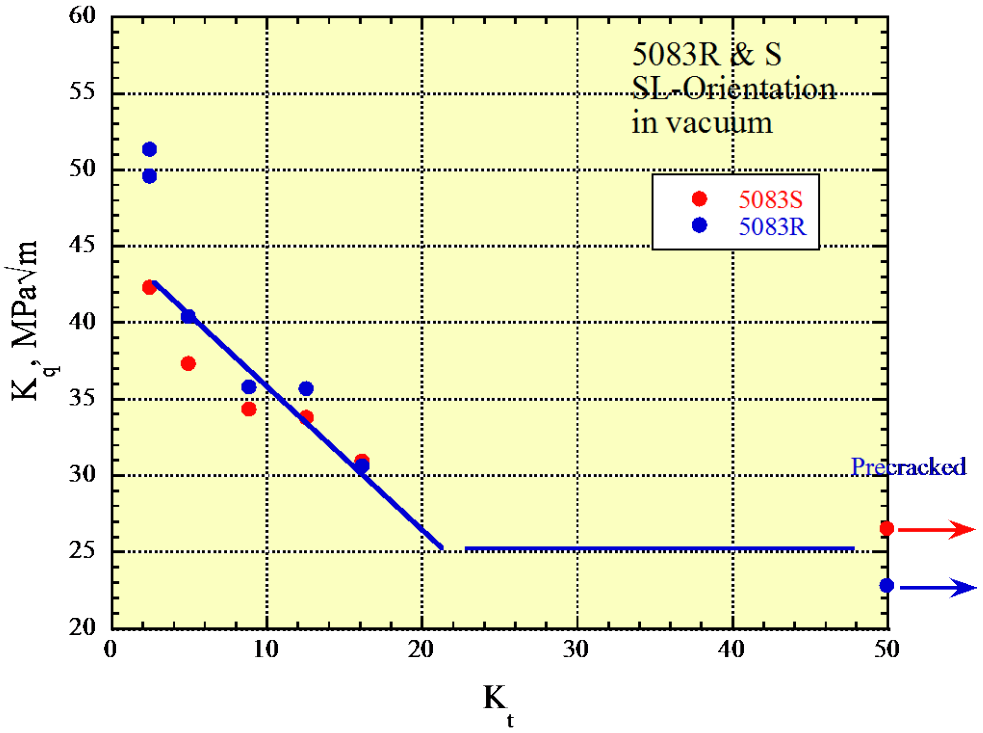

Figure A-9: Effect of K_t on fracture resistance of as-received Al 5083 (5083R) and sensitized Al 5083 (5083S) in vacuum.

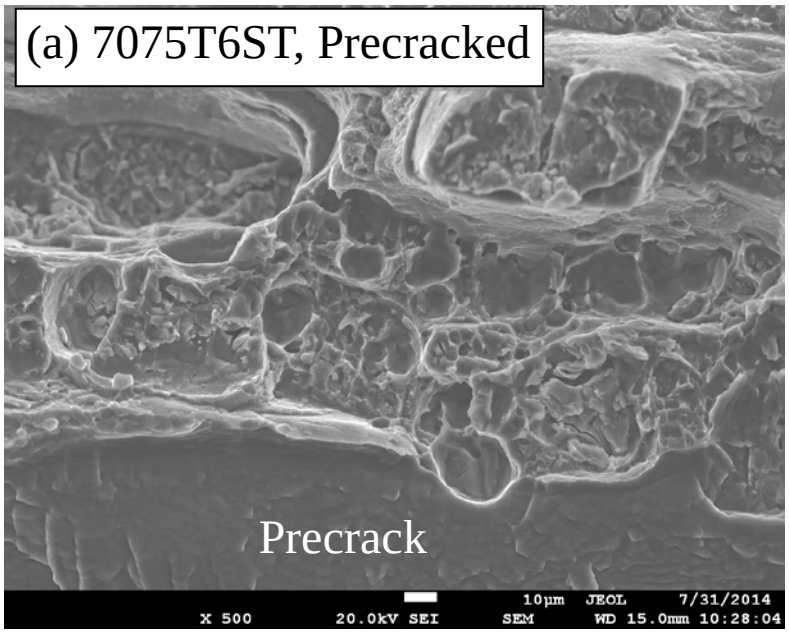

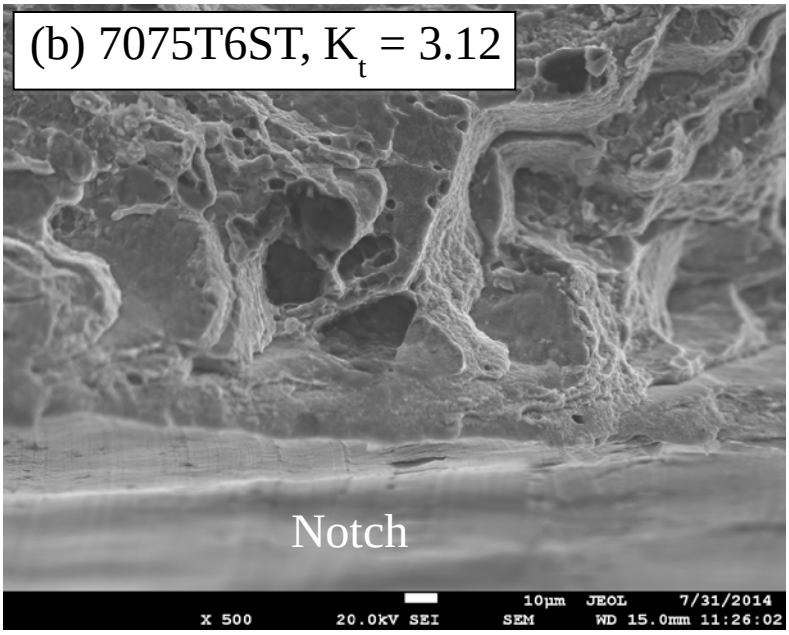

Figure A-10: Notch tip fracture surface morphology of peakaged 7075T651 in (a) fatigue-sharpened precracked specimen and (b) K_t = 3.12 blunt notch specimen.

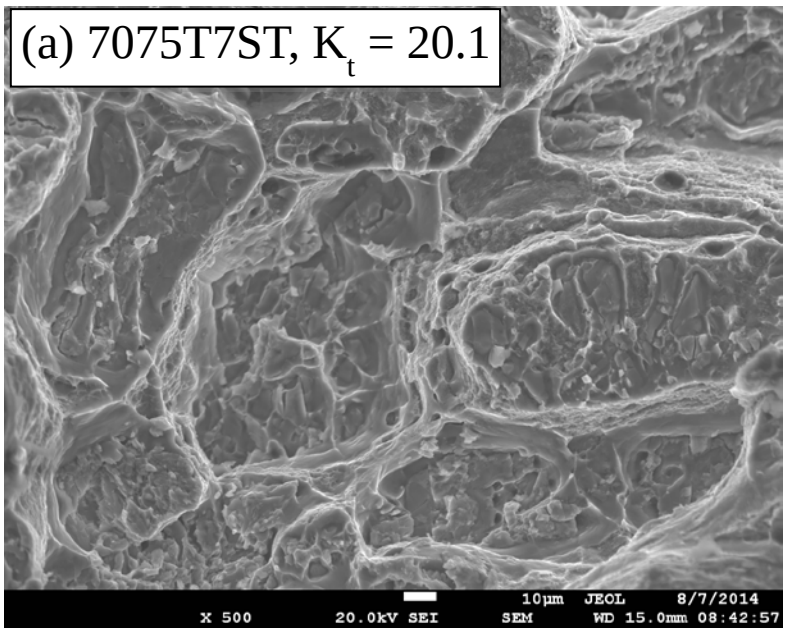

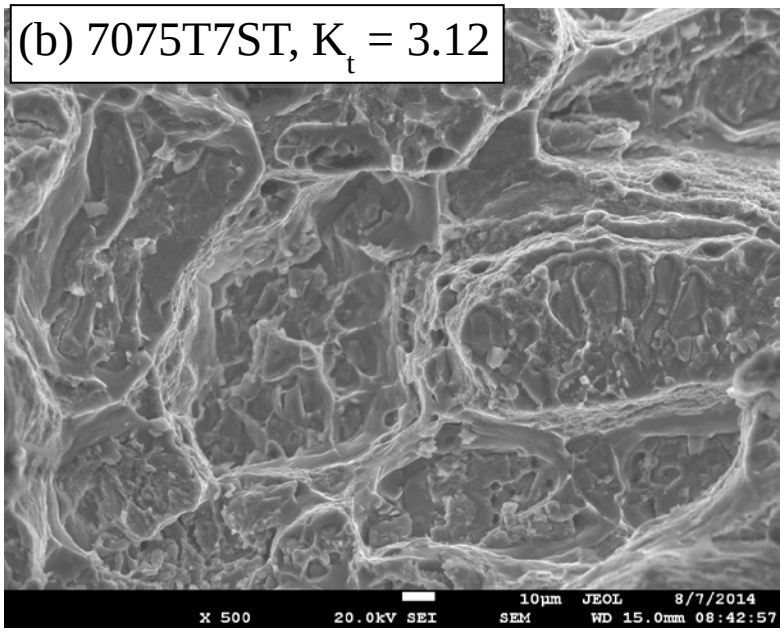

Figure A-11: Notch tip fracture surface morphology of overaged 7075-T7351 in (a) K_t = 20.1 sharp notch specimen and (b) K_t = 3.12 blunt notch specimen.